

Strain amplitude-dependent anelasticity in Cu–Ni solid solution due to thermally activated and athermal dislocation–point obstacle interactions

S. Kustov,^{a)} G. Gremaud, and W. Benoit

École Polytechnique Fédérale de Lausanne, Institut de Génie Atomique, CH-1015 Lausanne, Switzerland

S. Golyandin and K. Sapozhnikov

A. F. Ioffe Physico-Technical Institute, Politekhnicheskaya 26, 194021 St. Petersburg, Russia

Y. Nishino and S. Asano

Nagoya Institute of Technology, Showa-ku, Nagoya 466, Japan

(Received 20 February 1998; accepted for publication 14 October 1998)

Experimental investigations of the internal friction and the Young's modulus defect in single crystals of Cu-(1.3–7.6) at. % Ni have been performed for 7–300 K over a wide range of oscillatory strain amplitudes. Extensive data have been obtained at a frequency of vibrations around 100 kHz and compared with the results obtained for the same crystals at a frequency of ~ 1 kHz. The strain amplitude dependence of the anelastic strain amplitude and the average friction stress acting on a dislocation due to solute atoms are also analyzed. Several stages in the strain amplitude dependence of the internal friction and the Young's modulus defect are revealed for all of the alloy compositions, at different temperatures and in different frequency ranges. For the 100 kHz frequency, low temperatures and low strain amplitudes ($\sim 10^{-7}$ – 10^{-5}), the amplitude-dependent internal friction and the Young's modulus defect are essentially temperature independent, and are ascribed to a purely hysteretic internal friction component. At higher strain amplitudes, a transition stage and a steep strain amplitude dependence of the internal friction and the Young's modulus defect are observed, followed by saturation at the highest strain amplitudes employed. These stages are temperature and frequency dependent and are assumed to be due to thermally activated motion of dislocations. We suggest that the observed regularities in the entire strain amplitude, temperature and frequency ranges correspond to a motion of dislocations in a two-component system of obstacles: weak but long-range ones, due to the elastic interaction of dislocations with solute atoms distributed in the bulk of the crystal; and strong short-range ones, due to the interaction of dislocations with solute atoms distributed close to dislocation glide planes. Based on these assumptions, a qualitative explanation is given for the variety of experimental observations.

© 1999 American Institute of Physics. [S0021-8979(99)03802-5]

I. INTRODUCTION

Dislocation-point obstacle (PO) interactions are traditionally considered as basic to the amplitude-dependent internal friction (ADIF) in crystals (see Refs. 1 and 2, and references therein), although other structural scales could also be relevant, especially in the low-frequency range.^{3–7} Random solid solutions are inviting materials for experimental and theoretical investigations of the dislocation-PO interaction-related internal friction (IF), since they often suggest *a priori* information on the PO concentration and the binding energy with a dislocation, or even rule out the applicability of certain IF models. For instance, the classical oscillating string and the string breakaway Granato and Lücke models⁸ are usually considered impractical in the case of concentrated solid solutions,^{9–12} where the distance between solute atoms is comparable with the Burgers vector magnitude. From a theoretical standpoint the ADIF in random solid

solutions is traditionally considered to be due to motion of dislocations in an array of obstacles, randomly distributed in a glide plane.^{2,13–19} When the overcoming of obstacles by dislocations is thermally assisted, the existence of a relaxational maximum is predicted in the strain amplitude, temperature and frequency domains. Maxima of this type have been reported in temperature and strain amplitude domains for Cu–Al alloys^{20,21} and for Zr (Ref. 16) in the Hz and low kHz ranges, respectively.

The origin of the low-strain amplitude IF background is less well understood. A considerable amount of work, done since the early 1950s, has shown that the low-amplitude IF background in different materials is nearly frequency independent in the kHz range,^{22–27} and is orders of magnitude higher than that predicted by the oscillating string Granato-Lücke model. Several models were suggested to explain the weak frequency dependence and the high values of the low-amplitude IF background.^{13,19,28} Quite remarkable is a comparison of the results in Refs. 19 and 28. To explain the high values of the IF background in solid solutions in the low-frequency range, Gremaud²⁸ has suggested that the hysteretic

^{a)}Permanent address: A. F. Ioffe Physico-Technical Institute, 194021 St. Petersburg, Russia; electronic mail: Koustov@igahpse.epfl.ch

(frequency-independent) low-amplitude IF background in solid solutions originates from the long-range interaction of dislocations with elastic stress fields of obstacles situated away from the dislocation glide plane. In this case, the IF background is weakly strain amplitude dependent and a transition to the strongly amplitude-dependent IF occurs when dislocations overcome strong short-range obstacles distributed close to the glide plane (within the dislocation core). Distinguishing between two types of dislocation interactions with obstacles having the same origin also permitted the author to explain the regularities of the “peaking effect” during irradiation of crystals.^{2,28} In a recent theory of the IF in solid solutions, D’Anna *et al.*, on the contrary, neglected elastic interactions and considered solely the thermally assisted interaction of mobile dislocations with an array of obstacles distributed in a glide plane.¹⁹ They concluded that, at frequencies well below the dislocation-phonon relaxation maximum (~ 10 – 100 MHz), a purely strain amplitude-independent IF should exist due to the thermally activated dislocation-PO interactions. This amplitude-independent IF increases weakly with decreasing frequency, as opposed to the oscillating string Granato-Lücke theory, and transforms into the ADIF with increasing strain amplitude. Thus, completely different approaches with respect to dislocation-PO interactions have been employed^{19,28} to account for the same phenomenon. Clearly, the issue needs detailed experimental verification.

The problem of thermally activated and athermal dislocation microplasticity is relevant also to the general concept of the ADIF. Here, the ADIF frequency dependence is the basic challenge. According to Ref. 29, Kelvin was the first to study the frequency dependence of the ADIF, using torsional oscillations of wires. His data were irregular; nevertheless, the conclusion was drawn that the frequency dependence of the ADIF is weak. Since that time, numerous attempts have been undertaken to obtain convincing results concerning the ADIF frequency dependence. Read³⁰ reported that the ADIF in Zn single crystals was very nearly inversely proportional to the frequency of longitudinal vibrations at 38 and 76 kHz. On the other hand, Nowick²² and Takahashi²³ did not observe frequency dependence of the ADIF, employing resonant longitudinal and flexural oscillations for single and polycrystalline Cu, respectively. Hiki also reported that the ADIF in lead was independent of the vibration frequency in the kHz range.³¹ Recently, the frequency dependence of the ADIF has been studied at room temperature over a wide range of frequencies from infrasonic to ultrasonic for a number of crystals by means of several techniques, including direct registration of the dislocation anelastic strain.^{6,7,32} The conclusion has been drawn that the ADIF does depend on frequency, and that it is determined by contributions by different, but interrelated, mechanisms, both athermal and thermally activated ones. However, results on the combined influence of the temperature and frequency of vibrations on the ADIF are still lacking.

In this article we report the results of experimental investigations of the ADIF and low-amplitude IF background for Cu-Ni alloys of varying Ni contents, performed over wide strain amplitude and temperature ranges. Extensive

data are obtained at a frequency near 100 kHz and compared with results in the low-kHz range. The Cu-Ni system was selected for the experimental study due to the complete solid solubility of its components. Another advantage is the absence of a time dependence of the IF in Cu-Ni alloys at low and moderate temperatures, indicating the lack of PO mobility and segregation of solute atoms. Therefore, the Cu-Ni system provides a nearly perfect example of a random solid solution. In the present work we give a qualitative explanation for the variety of experimental observations based on the concept of dislocation motion in a two-component array of the PO. In Ref. 33, we suggested a microscopic model that accounts for both thermally activated and athermal contributions to dislocation microplasticity in solid solutions. The model predicts IF behavior which is in good agreement with the experimental data over the range of low, moderate and high strain amplitudes. The influence of temperature, frequency and alloy composition on the IF, qualitatively predicted by the model, also corresponds with available data and the results of the present research.

II. EXPERIMENTAL DETAILS

A. Internal friction measurements

The strain amplitude dependence of the IF and the Young’s modulus defect for 7–300 K was measured by means of the piezoelectric composite oscillator technique,³⁴ using longitudinal oscillations at a frequency of about 100 kHz. Specimens were cooled/heated in a He atmosphere under pressure of ~ 10 kPa with a cooling/heating rate of approximately 1 K/min. A computer-controlled setup³⁵ permitted measurement of the continuous temperature spectra of the IF and resonant frequency of the oscillator for two selected magnitudes of the oscillatory strain. The two values of the strain amplitude were stabilized in turn for each temperature step (1 K) and were usually selected to fall within apparently strain amplitude-independent and strain amplitude-dependent ranges. The difference between the IF at high and low strain amplitudes gives the strain amplitude-dependent part of the total IF. The strain amplitude dependence of the IF and resonant frequency, in the strain amplitude range of approximately 10^{-7} – 10^{-4} , was taken at selected temperatures during the same cooling/heating run. In the present work only the strain amplitude dependence of the IF and the Young’s modulus is considered in detail. During the measurements of the strain amplitude dependence the oscillatory strain amplitude was first increased with a preset step from the lowest value, and then decreased in a reverse sequence. It took approximately 1–2 min (depending on the number of points) to measure a strain amplitude dependence of the IF during cooling/heating of the specimen. The measurements of the strain amplitude dependence during cooling and heating gave essentially similar results for prestrained samples.

The decrement of the specimen, δ_s , was determined from the total measured decrement of the composite oscillator, δ_t , and the decrement of the quartz transducer alone, δ_q : $m_s \delta_s + m_q \delta_q = m_t \delta_t$, where m_s , m_q , and m_t are masses of a specimen, quartz transducer, and the total mass of the oscillator, respectively.³⁴ Before experiments with the com-

posite oscillator the temperature dependence of the IF in the quartz transducer alone was measured at different strain amplitudes. The decrement of the transducer alone changed from $\sim 10^{-4}$ at room temperature to $\sim 4 \times 10^{-5}$ at 7 K. The IF of the transducer did not exhibit strain amplitude dependence in the investigated range of strain amplitudes.

The IF was measured also at a frequency near 800 Hz by means of free decay of flexural oscillations.¹² Modification of the previous experimental setup,¹² including computer control and recording, enabled one to perform the measurements with higher precision and in a wider strain amplitude range.

B. Material and preparation of specimens

Cu-Ni alloys with different Ni contents (1.3, 2.3, 3.2, and 7.6 at. %) were prepared from 99.999% Cu and 99.998% Ni by melting them in an argon arc furnace. Single crystals with dimensions of $1.5 \times 10 \times 120$ mm were grown from seeds by the Bridgman technique in an argon atmosphere in graphite molds. Plate-shaped crystals with a surface parallel to the (111) plane were oriented for single slip (Schmid factor 0.45–0.49). Specimens with dimensions of $1.5 \times 10 \times 80$ and $1.5 \times 2 \times 18$ mm for the free decay and for the composite oscillator techniques, respectively, were spark cut from the grown crystals. The specimens were annealed in vacuum at 973 K for 20 h and then furnace cooled. The strain amplitude dependence was measured first for the annealed specimens. Then the specimens were deformed, without regluing them to a quartz transducer, into three-point bending to a sag of 0.05 mm with a span between the lower deforming fixtures of 11 mm.

III. EXPERIMENTAL RESULTS

A. Influence of temperature on the strain amplitude dependence of the internal friction

Figure 1 shows the strain amplitude dependence of the IF, taken at ambient and low, 7–11 K, temperatures for the prestrained specimens with different Ni contents. The curves corresponding to a strain amplitude increase (forward run) and decrease (reverse run), as indicated by arrows, are depicted in Figs. 1(a) and 1(b). Clearly, the direct and reverse runs of the strain amplitude dependence coincide fairly well at both low and ambient temperature. This observation indicates the stability of the structure, related to the ADIF, and allows one to exclude dislocation multiplication by ultrasound. Indeed, dislocation multiplication by vibrations, contrary to our data, is accompanied by a pronounced strain amplitude hysteresis (the ADIF on the reverse run of the strain amplitude dependence is higher than on the forward one).^{36–38} For the sake of clarity, only one run (usually the forward one) will be treated hereafter.

As we reported earlier,^{39,40} the strain amplitude dependence of the decrement is exhibited for all of the alloy compositions in several stages, and are most clearly distinguished at low temperatures. Transitions between stages depend on the temperature and on the Ni content. Nevertheless, the strain amplitude dependence of the decrement can be separated into three typical ranges.

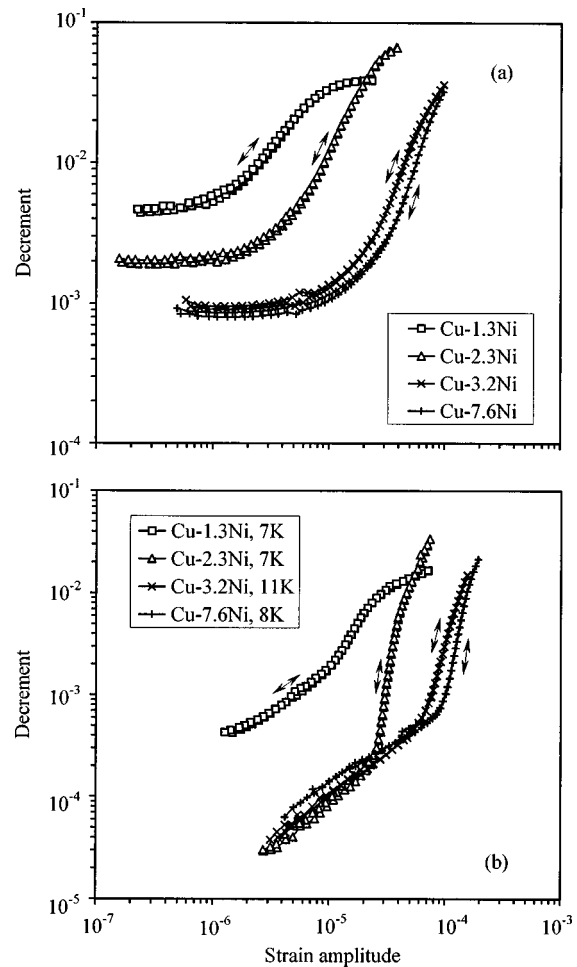


FIG. 1. Strain amplitude dependence of the decrement for specimens of Cu (1.3–7.6) at. % Ni crystals at room temperature (a) and at 7–11 K (b). All the results correspond to the prestrained specimens, except for an annealed Cu-2.3 at. % Ni specimen at 7 K.

1. Low strain amplitudes

At low temperatures [Fig. 1 (b)], the strain amplitude dependence shows no amplitude-independent range whatsoever. At the lowest strain amplitudes the strain amplitude dependence of the decrement δ_h can be fitted by power functions of strain amplitude ε_0 with an exponent $n \approx 0.7–0.8$:

$$\delta_h = F(c) \varepsilon_0^n, \quad (1)$$

where $F(c)$ is a function of the Ni content.

The independence of the stress exponent of the impurity content is to be noted. The low-amplitude stage is most pronounced for a Cu-7.6 at. % Ni crystal. The IF in the low-amplitude range at elevated temperatures will be examined in detail in Sec. III B.

2. Moderate strain amplitudes

The weakly amplitude-dependent part of the IF transforms here into a strongly amplitude-dependent one. This transition is very abrupt at low temperatures and high impurity concentrations, and becomes rather gradual with a temperature increase and for lower Ni content. This stage persists at both elevated and low temperatures for all of the alloys. Here, in contrast to the low-amplitude stage, the slope

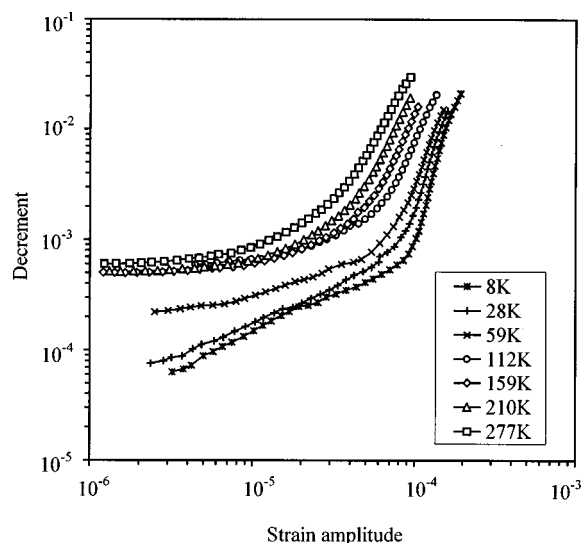


FIG. 2. Strain amplitude dependence of the decrement for a specimen of Cu-7.6 at. % Ni crystal for 8–277 K. The measurements were made during cooling.

of the strain amplitude dependence increases significantly with the impurity content, Fig. 1(b). It also reaches very high values at low temperatures for the annealed state of a Cu-2.3 at. % Ni specimen.

3. High strain amplitudes

Here, the strain amplitude dependence exhibits a tendency toward saturation, more or less pronounced, depending on the temperature and the alloy composition.

As for the general tendency, Figs. 1(a) and 1(b) show that the typical strain amplitudes of transition from one stage to another are shifted to higher strain amplitudes with decreasing temperature and increasing impurity content.

B. Analysis of the low-amplitude internal friction background and the Young's modulus defect at 100 kHz

The transformation of the low-amplitude stage of the strain amplitude dependence with temperature can be traced in Fig. 2. Here, the strain amplitude dependence taken at different temperatures is depicted for the Cu-7.6 at. % Ni alloy, where this stage is the most pronounced and covers at low temperature the strain amplitude range approximately from 10^{-6} to 10^{-4} . Figure 2 indicates that this prolonged stage changes to a seemingly amplitude-independent IF at 160 K and above. For the lowest strain amplitudes, $\sim 10^{-6}$, the background IF increases approximately an order of magnitude from 8 to 277 K.

In order to examine the initial part of the strain amplitude dependence in more detail, the curves from Fig. 2, at strain amplitudes below 1.5×10^{-5} , are depicted in Fig. 3 on a linear scale. Most remarkable is the fact that the IF is amplitude dependent and the slope of the strain amplitude dependence are likely to be the same in the range, 8–210 K. At elevated temperatures, 159 and 210 K, deviation from this regularity is observed at a strain amplitude of $\sim 10^{-5}$. This is due to the fact that the initial part of the second ADIF

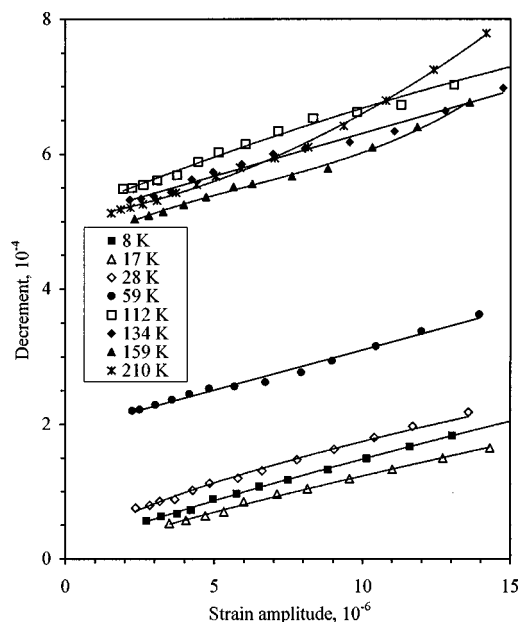


FIG. 3. Strain amplitude dependence of the decrement for a specimen of Cu-7.6 at. % Ni crystal (the same as in Fig. 2) for temperatures of 8–210 K and strain amplitudes 10^{-6} – 1.5×10^{-5} .

stage shifts to lower strain amplitudes with a temperature increase and falls within the depicted range. Thus, it appears reasonable to suggest that the low-amplitude part of the strain amplitude dependence is formed by two components: one weakly dependent on the strain amplitude, but independent of temperature; this component is responsible for the constant slope of the strain amplitude dependence at different temperatures; one amplitude-independent, but temperature-dependent, which is responsible for the parallel shift of the strain amplitude dependence at different temperatures, Fig. 3. This regularity can be traced for all of the alloy compositions, except Cu-1.3 at. % Ni, where the second stage of the ADIF is shifted at elevated temperatures to the lowest strain amplitudes investigated, making the low-amplitude stage barely detectable.

The following procedure was used for further ADIF analysis. The IF component, depending on temperature but not on strain amplitude, was subtracted from all the strain amplitude dependences of the decrement taken at elevated temperatures. For each temperature, the criterion for selecting the subtracted value was the best fit of the low-amplitude stage of the curve (Fig. 3) with the strain amplitude dependence, taken at the lowest temperature. The results of this procedure are represented in Fig. 4. This procedure is somewhat arbitrary for the Cu-1.3 at. % Ni alloy close to room temperature, since, as mentioned before, the low-strain amplitude stage of the ADIF cannot be detected accurately here. The results in Fig. 4 show clearly that, for each alloy composition, a single low-temperature asymptote for all of the strain amplitude dependence curves exists in the low-amplitude range. For all of the alloy compositions, there is a transition stage to a pronounced strain amplitude dependence of the IF. Two observations related to this transition stage merit attention. First, the onset of the deviation from the asymptotic low-temperature ADIF curve shifts to lower

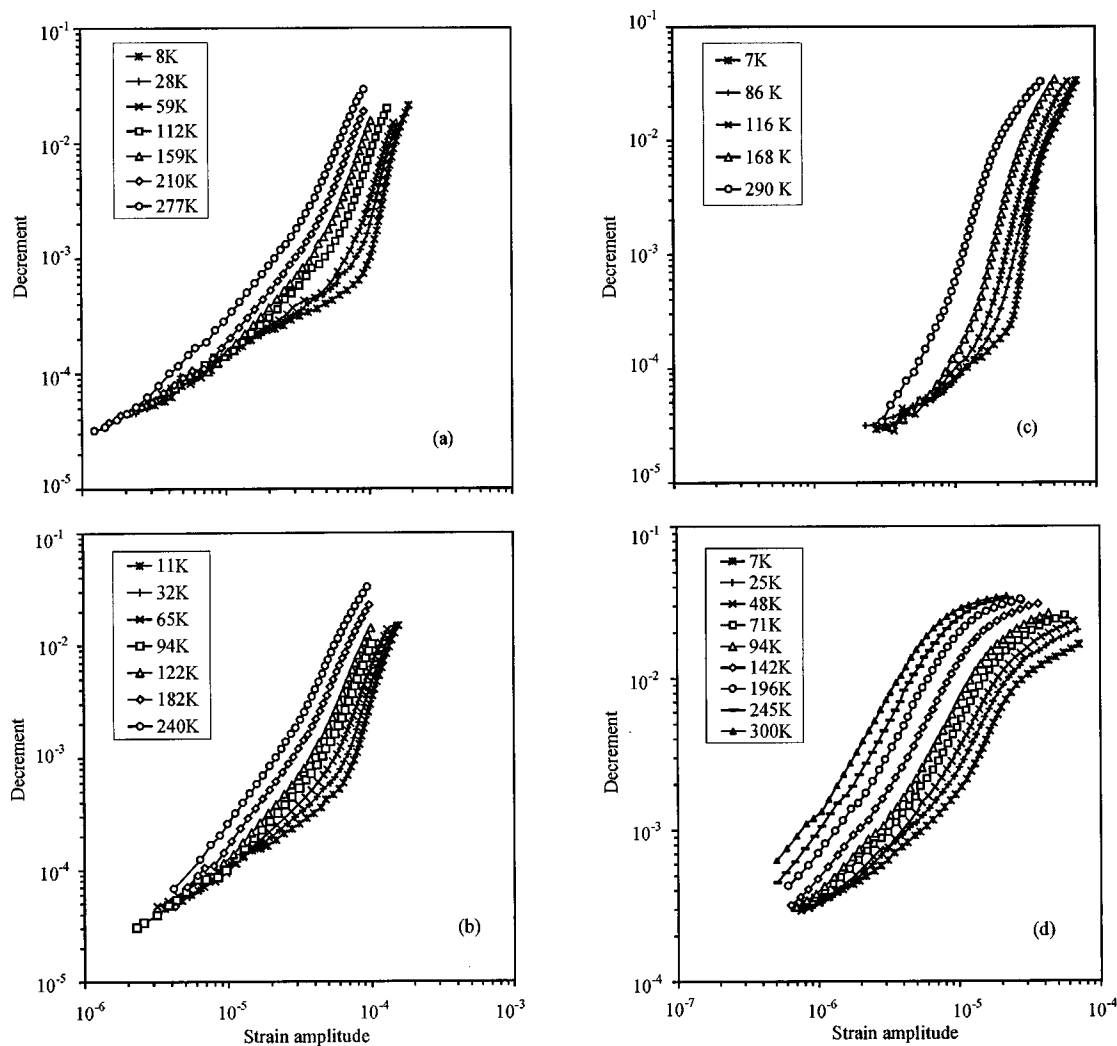


FIG. 4. Strain amplitude-dependent part of the decrement for specimens of Cu-7.6 at. % Ni (a), Cu-3.2 at. % Ni (b), Cu-2.3 at. % Ni (c) and Cu-1.3 at. % Ni (d) crystals for temperatures of 8–300 K. All the results correspond to the prestrained specimens, except for an annealed Cu 2.3 at. % Ni specimen. The measurements were made during cooling (a), (c) and heating (b), (d).

strain amplitudes with the decrease of the impurity content. Second, this transition is very abrupt at low temperatures and becomes more gradual with increasing temperatures.

Figure 5(a) shows the strain amplitude dependence of the Young's modulus defect for a Cu-7.6 at. % Ni specimen corresponding to the IF data in Fig. 4(a). Since the amplitude-independent modulus defect is not known, only the amplitude-dependent part of the modulus defect can be obtained. The amplitude-dependent Young's modulus defect (ADMD), $\Delta E/E$, is conventionally derived from the resonant frequency of a specimen f , which depends on the strain amplitude ε_0 : $(\Delta E/E)(\varepsilon_0) = 2[f_i - f(\varepsilon_0)]/f_i$, where f_i is the resonant frequency of a specimen in the strain amplitude-independent range. In the present results, the strain amplitude-independent range was not revealed for the resonant frequency, as was also true for the IF data. Therefore, the resonant frequency of a specimen at the lowest strain amplitude was assumed to be f_i . This substitution, evidently, may lead to an underestimation of the value of the ADMD, especially at the lowest strain amplitudes, but cannot influence the general regularities substantially, since the data

were taken in a wide strain amplitude range. The data in Fig. 5(a), apart from the lowest strain amplitudes which are obscured by the necessary procedure of deriving the ADMD, correspond perfectly with the regularities revealed in the strain amplitude dependence of the decrement. The existence of a similar low-temperature asymptote, weakly dependent on the strain amplitude, is obvious. The deviation of the ADMD from this asymptote with increasing temperature is very much like that for the strain amplitude dependence of the decrement. Since the ADMD represents an independent parameter, these results provide evidence of the correctness of the procedure used to derive the amplitude-dependent part of the IF in Fig. 4.

Figure 5(b) shows the strain amplitude dependence of the in-phase component of the anelastic strain amplitude for the Cu-7.6 at. % Ni specimen obtained from the strain amplitude dependence of the modulus defect:

$$\varepsilon_{\text{an}}(\varepsilon_0) = \frac{\Delta E}{E}(\varepsilon_0)\varepsilon_0. \quad (2)$$

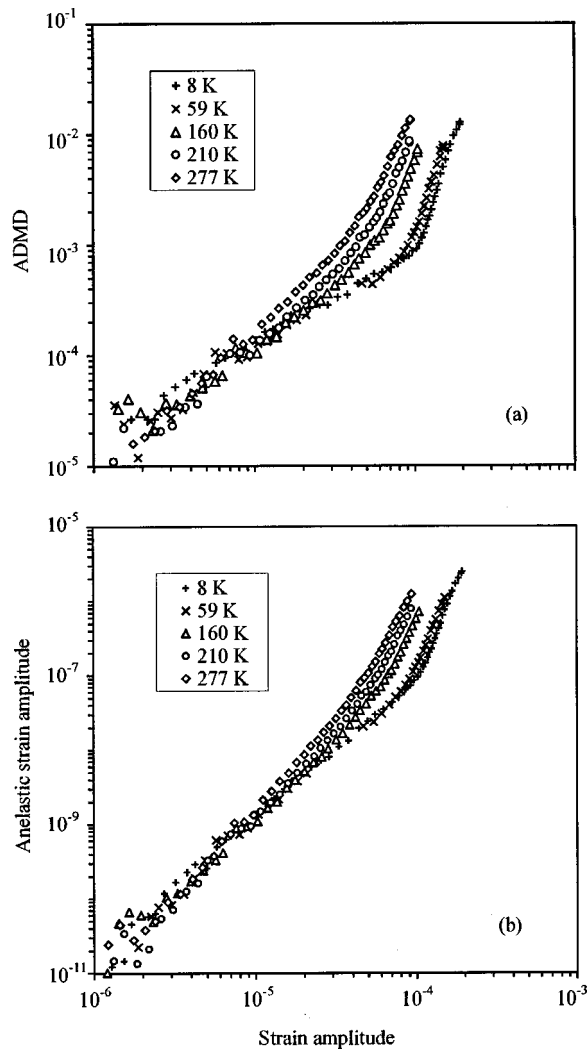


FIG. 5. Strain amplitude dependence of the Young's modulus defect (a) and anelastic strain amplitude (b) for a specimen of Cu-7.6 at. % Ni crystal for 8–280 K. The measurements were made during cooling.

The data in Fig. 5(b) demonstrate that the temperature-independent and weakly strain amplitude-dependent IF component covers, at low temperatures, the range of anelastic strain exceeding three orders of magnitude.

Summarizing Sec. III B, we identify the low-amplitude IF background observed in the present work as a sum of two components: a purely strain amplitude-independent, but temperature dependent IF component; a weakly strain amplitude-dependent IF component, the key feature of which is temperature independence at ultrasonic frequencies and low temperatures.

C. Comparison of the internal friction data at 1 and 100 kHz

Figure 6 shows the influence of frequency on the strain amplitude dependence of the decrement for the annealed Cu-3.2 at. % Ni and Cu-1.3 at. % Ni specimens. Apparently, both the low-amplitude IF background and the ADIF at the high-amplitude stage are substantially higher at a frequency around 1 kHz than in the 100 kHz range. The results for the same specimens measured at ~100 kHz after prestrain are

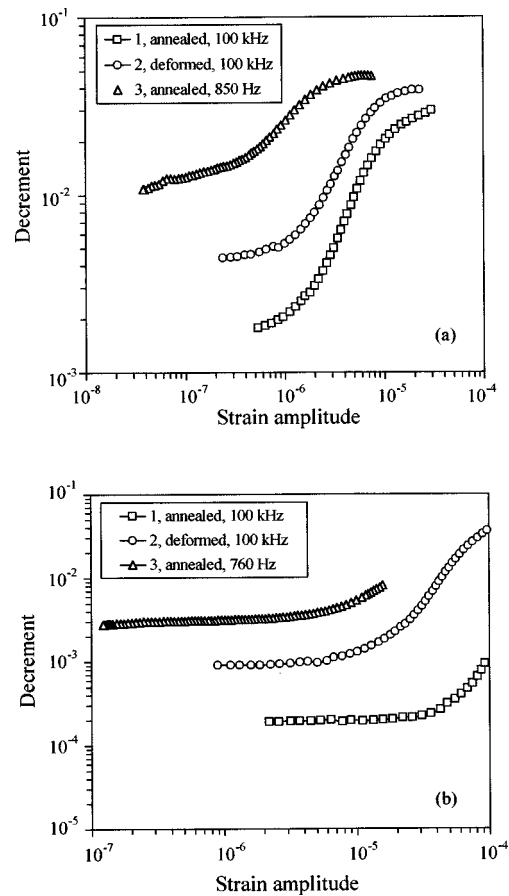


FIG. 6. Strain amplitude dependence of the decrement at room temperature for specimens of Cu-1.3 at. % Ni (a) and Cu-3.2 at. % Ni (b) crystals for the annealed state (1), (3) and after prestrain (2) at frequencies of ~100 (1), (2) and ~1 kHz (3).

displayed as well and show a considerable increase with prestrain of the IF for all stages of the strain amplitude dependence. Several remarks are necessary here concerning the comparison of the data obtained by different techniques and for different specimens.

First, one cannot exclude accidental cold-working of the specimens during handling and mounting procedure. Such cold-working can change the IF values considerably (see Fig. 6). To rule out this source of uncertainty, a comparison between the specimen in the annealed state at ~1 kHz and an intentionally deformed specimen at 100 kHz shows that the IF for all of the stages is still notably higher in the sonic range than at ultrasonic frequencies (see Fig. 6). An essential detail is that prestraining of specimens mostly influences the absolute value of the low-amplitude IF and ADIF, whereas typical strain amplitudes of the transition from one stage to another are changed only slightly; see the curves for 100 kHz in Fig. 6. Decreasing the frequency below 1 kHz influences the absolute values of the damping and noticeably shifts the transition stages of the ADIF to significantly lower values of strain amplitude.

Second, the thermoelastic relaxation should be considered as a possible contributor to the amplitude-independent IF component in the kHz range. The time constant τ and the

relaxation amplitude Δ for simple bending of a thin rectangular bar are given by^{1,41}

$$\tau = a^2 C_p \rho / (\pi^2 k_t),$$

$$\Delta = E \alpha^2 T / (\rho C_p),$$

where a is the specimen thickness, C_p the heat capacity, ρ the density, k_t the thermal conductivity, E the Young's modulus, α the thermal expansion coefficient, and T the temperature.

The estimations performed for the present geometry of a specimen show that (i) the maximum of the thermoelastic relaxation is expected at frequencies of 80, 37 and 13 Hz for pure Cu, Cu-2 wt % Ni and Cu-10 wt % Ni alloys, respectively, and (ii) the decrement value at a frequency of corresponding relaxation maxima at room temperature for all of the alloy compositions should be of the order of 5×10^{-3} . The C_p , ρ , k_t , and α values for Cu and for Cu-Ni alloys were taken from Ref. 42. Since the thermoelastic relaxation maximum is expected at frequencies 20–40 times lower than the 800 Hz employed in the present work, the thermoelastic damping is at least an order of magnitude lower than the measured low-amplitude IF level.

We mention here as well that the amplitude-independent apparatus background at ~ 1 kHz is also at least an order of magnitude lower than the measured IF values, this lower value being necessary to observe the dramatic suppression of the IF background values with the increase of Ni content (see the present results, but for a wider range of Ni contents see Ref. 12).

Third, as far as the ADIF is concerned, the intrinsic damping of the material should be compared rather than the damping of specimens measured by different techniques.^{43,44} The conversion of the measured damping to the intrinsic one requires either a homogeneous or a well-known distribution of dislocations in the bulk of a specimen. This requirement cannot be met for prestrained specimens. A comparison of the intrinsic ADIF values in the 1 and 100 kHz ranges for annealed Cu-1.3 at. % Ni specimens was performed in Ref. 39, and the ADIF behavior, with a change of frequency, was the same as in the present work. Besides, it is evident from the data in Ref. 39 that the influence of the frequency change from ~ 800 Hz to 100 kHz is far in excess of the possible influence of the procedure of conversion to the intrinsic damping.

Thus, the conclusion can safely be drawn that the measured low-amplitude IF background and the ADIF are frequency dependent. Inasmuch as the IF on different stages of the strain amplitude dependence is strongly influenced by prestrain, this frequency-dependent IF is due to dislocations.

D. Origin of the strain amplitude-independent internal friction component

A question arises at this stage concerning the nature of the strain amplitude-independent component of the low-amplitude IF background, which was subtracted from the total damping to derive the amplitude-dependent part of the IF in Sec. III B. To clarify the source of this component, its temperature dependence has been analyzed. The results for

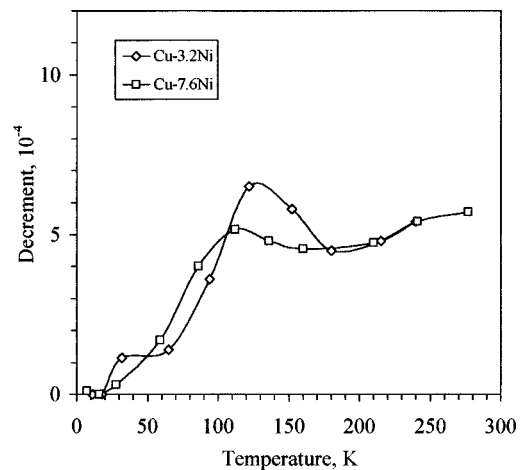


FIG. 7. Temperature dependence of the strain amplitude-independent internal friction component for Cu-3.2 at. % Ni and Cu-7.6 at. % Ni crystals.

Cu-7.6 at. % Ni and Cu-3.2 at. % Ni alloys are represented in Fig. 7. A maximum is observed in the temperature dependence of the amplitude-independent IF near 110 K. The position of this maximum corresponds rather well with the Bordoni relaxation [the B2 peak for copper is expected near 100 K for frequency of 100 kHz (Ref. 45)], clearly pointing to the dislocation origin for the amplitude-independent IF component, at least at the temperatures of Bordoni relaxation. However, the amplitude-independent component increases continuously at temperatures well above the temperature of the Bordoni relaxation. The influence of the prestrain on the IF, Fig. 6, can be used to verify the dislocation-related origin of the amplitude-independent IF at elevated temperatures. Evidently, the low-amplitude IF background increases considerably with prestrain. The amplitude-independent IF component constitutes a substantial part of the low-amplitude damping at room temperature. Therefore, the increase of the low-amplitude damping with prestrain is an indication of the dislocation nature of the amplitude-independent IF component at temperatures higher than that of Bordoni relaxation as well. There is a possibility that a significant part of the ultrasonic amplitude-independent IF in the ~ 100 kHz range, observed at temperatures above Bordoni relaxation, is due to the linear viscous friction component, described by the oscillating string model.⁸ The key issue here is very much like that for the ADIF, the frequency dependence of the amplitude-independent IF component. With regard to the frequency dependence of the low-amplitude IF background, it is quite remarkable to note that it increases with decreasing frequency to ~ 1 kHz, contrary to the expected contribution of the viscous oscillating string component.⁸ Unfortunately, the purely strain amplitude-independent component of the low-amplitude IF background at ~ 1 kHz and its frequency dependence cannot be derived from the present results. However, if the strain amplitude-independent IF component increases with the frequency decrease, that is likely because of a much higher low-amplitude IF background at ~ 1 kHz as compared to 100 kHz (see Fig. 6); it could be the evidence in

favor of the mechanism suggested for solid solutions by D'Anna *et al.*¹⁹ rather than the classical oscillating string model.⁸

E. Influence of temperature and frequency on the strain amplitude dependence of the internal friction

A comparison of the influence of temperature and frequency on the strain amplitude dependence of the decrement is shown in Fig. 8. Here, the strain amplitude dependences taken for Cu-1.3 at. % Ni and Cu-3.2 at. % Ni alloys at 100 kHz and at temperatures between 8 and 300 K are compared with those taken at room temperature and a frequency around 1 kHz. As mentioned before, the ADIF at ~ 1 kHz is substantially higher for all of the ADIF stages. We wish to make two important remarks here.

First, three observations describe the data at both frequencies: the weak strain amplitude dependence at low strain amplitudes, the stronger variation in the intermediate range, and the saturation at high strain amplitudes. At high temperatures the saturation transforms into a maximum for a Cu-1.3 at. % Ni crystal at a frequency of ~ 850 Hz, Fig. 8(a).

Second, an increase of the temperature and a decrease of frequency are equivalent in their action on both the absolute values of the ADIF and the transitions between the ADIF stages. This is a clear indication of a thermally activated process.

The insets in Fig. 8 show in more detail the behavior of the low-amplitude IF background at ~ 1 kHz on a linear scale of damping. Clearly, the IF is strain amplitude dependent over the entire strain amplitude range investigated. Moreover, it appears that the IF at low strain amplitudes may have its own substructure at low frequencies. For the Cu-3.2 at. % Ni alloy the IF increases noticeably at strain amplitudes from 10^{-7} to 3×10^{-7} . This increase becomes more gradual, exhibiting a kind of a plateau at 3×10^{-7} – 2×10^{-6} , and only then is followed by the second, steep ADIF stage.

IV. DISCUSSION

A. Comparison with available experimental data

The IF in crystals of the Cu-Ni system has been reported in Refs. 12, 39, 40, and 46. The measurements for Cu-(0.4–7.6) at. % Ni single crystals performed by Nishino *et al.*¹² at temperatures of 140–295 K in the ~ 1 kHz range covered a somewhat narrower strain amplitude range than that in the present work, and therefore only the strain amplitude-independent IF and a single stage of the ADIF were distinguished. The results were analyzed from the standpoint of a phenomenological approach,⁴⁷ permitting one to deduce the microyield stress from ADIF data. Gottschall and Beshers⁴⁶ investigated the strain amplitude dependence of the IF in Cu-(0–4) at. % Ni single crystals at a frequency ~ 22 kHz in the temperature range 95–297 K. The strain amplitude range corresponded to that of the present work and even slightly exceeded it at 95 K. However, the scatter of the data was considerable, and the damping values for a high Ni content alloy were “obscured by the limits of sensitivity of the apparatus” at the lowest temperature.⁴⁶ Perhaps, that is why the authors⁴⁶ did not observe the temperature-independent

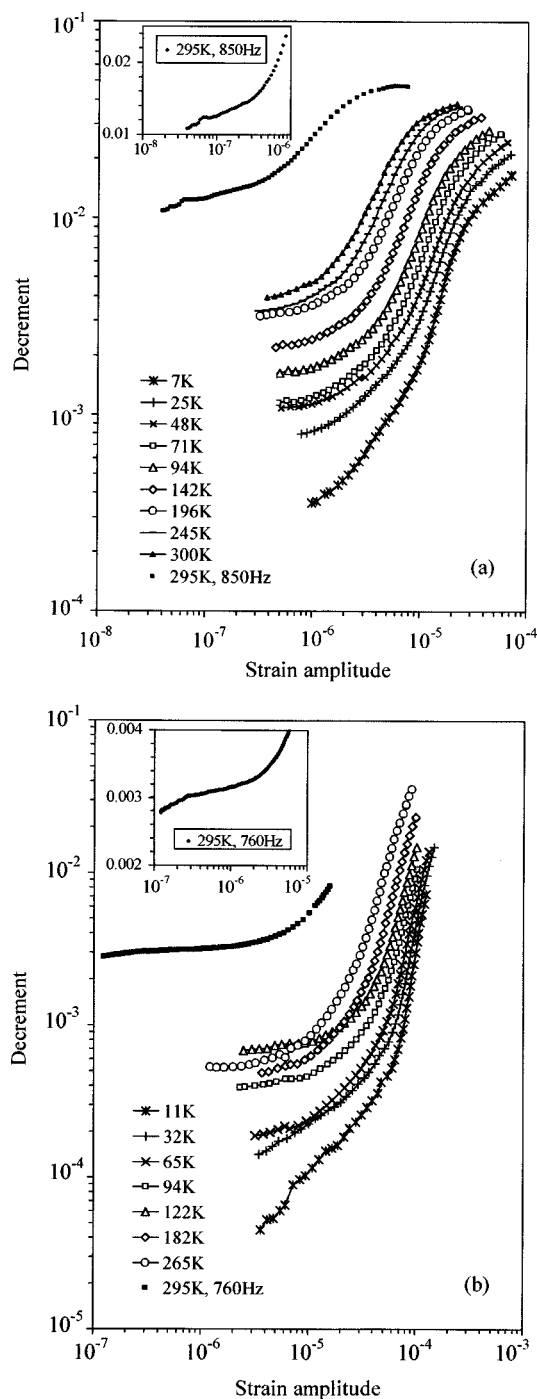


FIG. 8. Strain amplitude dependence of the decrement for prestrained Cu-1.3 at. % Ni (a) and Cu-3.2 at. % Ni (b) specimens for the range 7–300 K at a frequency of ~ 100 kHz. The strain amplitude dependences, taken at a frequency ~ 1 kHz for annealed specimens of the same compositions, are shown as well. The insets depict the initial parts of the strain amplitude dependences at ~ 1 kHz with a linear scale for the ordinates.

ADIF stage at low strain amplitudes, which is persistent in our results especially at the lowest temperatures and highest concentrations of Ni. Nevertheless, Gottschall and Beshers did distinguish two stages of the strain amplitude dependence: the temperature-dependent and the nearly temperature-independent stages at moderate and high strain amplitudes, respectively. The ADIF saturation and, sometimes, formation of the ADIF maximum at high strain am-

plitudes are persistent in their data⁴⁶ for all of the alloy compositions, although they did not mention this regularity. In our previous work,^{39,40} the strain amplitude dependence of the IF was measured *in situ* during deformation of Cu-Ni single crystals at room temperature. No qualitative influence of the deformation process on the ADIF was reported, pointing to the stability of the dislocation-PO structure due to low Ni atom mobility at low and moderate temperatures. The same stages as in the present work were observed in the strain amplitude dependence insofar as the ranges overlap.

The results of Jon *et al.*⁹ on the ADIF in α -brass with 20% and 35% Zn, obtained in a wide strain amplitude range at room temperature, are quite indicative. The authors⁹ revealed the same stages of the strain amplitude dependence, as in the present work: an amplitude-independent one at the lowest strain amplitudes, below approximately $(2-3) \times 10^{-5}$, depending on the composition, grain size and pre-history of the specimen (this range has an upper limit of $\sim 10^{-6}$ for pure copper); a weakly amplitude-dependent one at moderate strain amplitudes below approximately $(1-2) \times 10^{-4}$; a strongly amplitude-dependent one with a saturation at the highest strain amplitudes above $(1-2) \times 10^{-4}$. The stages were shifted to somewhat higher strain amplitudes, as compared to the present results, perhaps due to the higher content of the alloying element and its higher binding energy with dislocations.

Thus, the experimental data in the present work correspond well with previously performed research, but are much more comprehensive due to the wide temperature and strain amplitude ranges employed and the precision of the measurements.

B. Suggested mechanisms for the multistaged amplitude-dependent internal friction in Cu-based solid solutions

1. Low-strain amplitude range

We will consider below only the mechanisms suggested for the strain amplitude-dependent components of the IF. No specific mechanism was proposed for the weakly amplitude-dependent part of the strain amplitude dependence, observed by Jon *et al.*⁹ The authors supposed, however, that fluctuations in solute atom distribution, with spatial wavelength $\lambda > w_k$, where w_k is the kink width, are responsible for the strong pinning of dislocations, whereas single impurities provide much weaker pinning. The region of the weak strain amplitude dependence was identified as due to the unpinning of dislocations from weaker pinning points. As mentioned before, this stage has not been discerned by Gottschall and Beshers⁴⁶ or by Nishino *et al.*¹²

As for other materials, a similar weakly strain amplitude-dependent and essentially temperature-independent IF was observed in the β'_1 martensitic phase of Cu-Al-Ni crystals at a frequency of ~ 100 kHz.^{48,49} An explanation was suggested based on the Gremaud concept of the athermal interaction of dislocations with the PO distributed in the bulk.²⁸ A weakly strain amplitude-dependent IF was observed at low strain amplitudes in the kHz range in 99.999% Cu,⁵⁰ pure Au,²⁶ and Au-Pt dilute solid solutions.²⁷

Baur and Benoit^{26,27} reported that the low-amplitude IF background was practically temperature independent (200–300 K) and seemingly frequency independent (0.3–3 kHz). This low-amplitude IF background has been attributed to a kind of hysteretic interaction of dislocations with point defects, different, however, from the dislocation breakaway.^{26,27} Lauzier *et al.*⁵⁰ ascribed the amplitude dependence of the low-amplitude IF background, at least in the region of Bordoni relaxation, to the nonlinear properties of the kink pair formation mechanism.

The substructure of the low-amplitude IF background was revealed both in pure Cu and in Au-Pt solid solutions. The IF rose steeply below a strain amplitude of $\sim (1-3) \times 10^{-7}$, and then slowly increased at higher strain amplitudes.^{27,50} This regularity corresponds with our data at a frequency of ~ 1 kHz; see Fig. 8. Quite remarkable was their observation that the stage of the initial increase of the IF background shifted to higher strain amplitudes with decreasing temperature.^{27,50} This fact apparently contradicts the suggestion of a purely athermal hysteretic mechanism for the low-amplitude IF background.^{26,27,51}

The present results clearly indicate that the weakly amplitude-dependent IF stage at low strain amplitudes is persistent for different alloy compositions over wide ranges of temperature and frequency. Comparison with the available data shows that this low-amplitude ADIF stage is characteristic of solid solutions of different compositions as well as of rather pure face-centered-cubic (fcc) metals. Other data^{48,49} show that weakly strain amplitude-dependent athermal IF also persists in a wide range of strain amplitudes and attains very high values in the low-symmetry martensitic phase of Cu-Al-Ni crystals. Thus, one comes up against a rather general phenomenon, a model for which is still lacking.

The most salient feature observed in the present work, one which should be used to suggest an explanation, is the temperature independence of the low-amplitude ADIF component at ultrasonic frequencies, ~ 100 kHz, and low temperatures; see Figs. 4 and 5. Decreasing the frequency to the 1 kHz range and increasing the temperature lead to the formation of a low-amplitude IF background with typical substructure, as previously reported.^{26,27,50} To obtain an explanation of this effect, we intend to analyze in more detail the transition stage between the temperature-independent low-amplitude ADIF and the strongly amplitude-dependent stage at higher strain amplitudes.

The observed regularities in the behavior of the low-amplitude ADIF stage can be explained self-consistently based on the Gremaud model of the athermal hysteretic IF background,^{2,28} accounting for the dislocation-strong obstacle interaction as well. According to the Gremaud model, an adequate description of dislocation-PO interactions should consider the PO as distributed in the bulk of a crystal.^{2,28} With respect to a gliding dislocation, obstacles situated close to the dislocation glide plane represent strong short-range obstacles, which can be overcome with the assistance of thermal fluctuations. Those obstacles which lie apart from the glide plane interact elastically with a dislocation. This weak elastic interaction is long range. Because of the very large activation distances, weak obstacles can be over-

come only athermally. Following Refs. 2 and 28, the hysteretic interaction of a dislocation (with or without hard pinning points) with the weak long-range obstacles is at the origin of the low-amplitude athermal (temperature- and frequency-independent) and weakly strain amplitude-dependent IF in solid solutions. At higher strain amplitudes, a transition to the thermomechanical breakaway from strong obstacles was predicted.²

The low-temperature behavior of Cu-Ni crystals and the Cu-Al-Ni alloy at a frequency of ~ 100 kHz is in qualitative agreement with the predictions of the Gremaud model. However, the model^{2,28} considers, at the low-amplitude stage, interactions of dislocations solely with weak long-range obstacles. Therefore, the hysteretic low-amplitude IF is expected to be purely temperature and frequency independent. In the present work the deviation of the IF with increasing temperature from the single low-temperature asymptote is observed to shift over a wide range of strain amplitudes, Fig. 4. This clearly indicates that the interaction of mobile dislocations with strong obstacles already occurs in the strain amplitude range, where the low-amplitude ADIF is purely hysteretic at low temperatures. Thus we conclude that, in the range of strain amplitudes investigated, ***dislocation motion in a two-component system of obstacles should be considered rather than pure hysteretic interaction solely with weak long-range obstacles.***^{2,28}

Dislocation motion in a two-component system of obstacles has been investigated theoretically; see, for example, Ref. 52. However, usually weak obstacles were considered as due to short-range dislocation-PO interactions. The strong obstacles were ascribed to the interactions of a mobile dislocation with forest dislocations.⁵² The weak obstacles were considered as thermally activated, but the strong ones as athermal at low and moderate temperatures. The fundamental difference between the approach used in the present work and previous ones is twofold. First, both weak (long-range) and strong (short-range) obstacles may have the same origin (for instance, substitutional atoms in solid solutions), their type being dependent on their position with respect to a gliding dislocation. Second, the nature of the obstacles with regard to thermal activation is inverted compared with the conventional approach. Namely, weak obstacles are considered as athermal, whereas the strong ones require thermal activation. Keeping in mind these preliminary considerations, we will consider three typical (with respect to temperature and frequency) ranges. We restrict our attention here to the range of moderate stress amplitudes, well below the critical stress for a long-range dislocation motion in an array of obstacles.

a. Low temperatures, high frequencies. Here, at low and moderate strain amplitudes, dislocations overcome only weak obstacles. Strong obstacles restrict dislocation motion, and they are not penetrable in short times at low temperatures. At the present stage it is irrelevant whether dislocations are initially pinned or encounter strong obstacles while moving. However, it is a reasonable assumption that thermally activated obstacles in this domain represent strong pinning points, thus determining the average length of a mobile dislocation segment.

Experimentally, this type of low-amplitude IF behavior is observed at low temperatures in the present work for Cu-Ni crystals and in the Cu-Al-Ni alloy.^{48,49}

b. Moderate temperatures and intermediate frequencies. In this range, overcoming a progressively larger amount of strong short-range obstacles becomes possible (due to the thermal energy) in the most favorable dislocation configurations. Still, weak long-range obstacles also impede dislocation motion. From the standpoint of dislocation motion in a two-component array of obstacles, this is the most complicated region, where overcoming the strong and weak obstacles is strongly interrelated. Here we suggest that, at low and moderate strain amplitudes, when the temperature is increased or the frequency decreased, a certain number of strong obstacles are so situated as to be overcome during the course of a stress maximum, leading to an increase of the average length of a dislocation segment moving through weak long-range obstacles.

At 100 kHz, this region corresponds to the temperature- and frequency-dependent transition stage from the purely hysteretic background to the strongly strain amplitude-dependent ADIF.

c. High temperatures, low frequencies. Here, thermal agitation reduces the average force due to short-range obstacles. Thus, the efficiency of athermal obstacles and thermal ones may become comparable. One expects that, in this range, the mobility of dislocations becomes, as it does for the low-temperature range, determined predominantly by weak long-range obstacles, since their concentration is much higher than that of the thermal ones. Thus, decreasing frequency and/or increasing temperature leads to limiting conditions where the hysteretic background model is again applicable. However, in contrast to the low-temperature/high frequency range, the average dislocation segment length becomes much longer, since short-range obstacles do not act as hard pinning points any more. Here, another level of defect structure determines the strong pinning points for a mobile dislocation, for instance, the nodes of a dislocation network. This leads to considerably higher values of the low-amplitude IF, which is expected to be slightly frequency and temperature dependent due to the action of retained thermally activated obstacles, but in the limit frequency and temperature independent.

Regularities related to the mechanism of the low-temperature and low-amplitude ADIF can be analyzed further on the phenomenological level. Figure 9 shows the strain amplitude dependence of the IF and ADMD for a Cu-7.6 at. % Ni crystal at 8 K. As mentioned before, the strain amplitude dependences of the IF and the modulus defect are qualitatively similar. This similarity can be expressed quantitatively through the value of the ADIF to ADMD ratio, $r = \delta_h / (\Delta E/E)$, also represented in Fig. 9. Apparently, the r value is nearly constant in a wide range of strain amplitudes, corresponding to the occurrence of the hysteretic IF background mechanism, and increases dramatically with the onset of the pronounced strain amplitude dependence. The ADIF data can be fitted in the range $3 \times 10^{-6} - 10^{-4}$ by a power function (solid line) with the exponent $n=0.7$; see Eq. (1). It has been shown for the unlo-

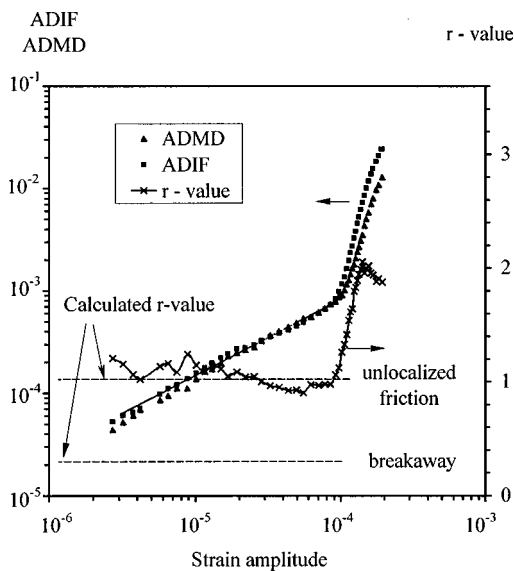


FIG. 9. Strain amplitude dependence of the decrement and the Young's modulus defect and their ratio r for a Cu-7.6 at. % Ni specimen at 8 K and frequency of ~ 100 kHz. The solid line represents the fitting of the decrement below a strain amplitude of 10^{-4} by the power function with a stress exponent $n = 0.7$.

calized friction model that a power law dependence of the anelastic strain ε_{an} on the applied stress σ ,

$$\varepsilon_{an}(\sigma) \propto \sigma^m, \quad (3)$$

yields^{53,54}

$$r = \frac{4n}{n+2}, \quad (4)$$

where $n = m - 1$ is the exponent in Eq. (1). Figure 9 represents also the r value calculated for the unlocalized friction static hysteresis and breakaway models according to Eq. (4) above and to Eq. (12) in Ref. 55, respectively. The experimental data show reasonable agreement with Eq. (4) up to strains of $\sim 10^{-4}$, and are obviously inconsistent with the calculation for the breakaway model. Thus, one concludes that, at low temperatures, the amplitude-dependent anelastic response of Cu-Ni crystals to the applied stress is, likely, close to the function of Eq. (3), corresponding to the hysteretic unlocalized friction model.

Thus we see that the behavior of the low-amplitude IF in different temperature and frequency ranges can be qualitatively accounted for by the motion of dislocations in a two-component system of obstacles. The suggestion which underlies this explanation is that the change of the strength of one type of obstacle with temperature/frequency leads to a change of the effective dislocation segment length.

The explanation of the low-amplitude IF behavior, based on the effective dislocation segment length, is strongly supported by the data for the Cu-Al-Ni alloy. Partial dislocations, bounding stacking faults, are the basic defects of the β'_1 martensitic structure.⁵⁶ The existence of long dislocation segments in the ordered network of partial dislocations in the β'_1 martensite was deduced from the large temperature anomaly of the Young's modulus, ascribed to the pinning of dislocations by mobile obstacles.^{48,49} Very high values of the

low-temperature IF background in Cu-Al-Ni crystals,^{48,49} similar to the pronounced anomaly of the Young's modulus, are consistent with the existence of long dislocation segments.

Thus, the mechanism of the low-amplitude ADIF stage may be conceived of as an athermal hysteretic one, with parameters (the average loop length is the principal one) controlled by a thermally activated process. The range of PO concentrations in which this hysteretic mechanism is efficient was reported to be very wide.^{2,28} Perhaps this gives an explanation for the observation of the hysteretic low-amplitude IF background in different, even rather pure, materials. Evidently, the overcoming of short-range obstacles also contributes to the low-amplitude IF at elevated temperatures. The contribution of the athermal and thermally activated events to the total low-amplitude IF depends on the frequency and the temperature. Estimation of this contribution is challenging, and beyond the scope of the present work.

2. Moderate and high strain amplitude range

Gottschall and Beshers⁴⁶ attributed the moderate strain amplitude stage of the ADIF in annealed Cu-Ni crystals to the thermomechanical breakaway of dislocations from combined Suzuki-Cottrell atmospheres. The temperature-independent (weakly temperature-dependent) part, corresponding to the saturation range of the ADIF, they ascribed to a hysteretic motion of dislocations over solute atoms located outside of the atmospheres. They suggested that dislocations are not retrapped by the atmospheres because of a high kinetic energy of dislocations that have broken away from the atmospheres.

The ADIF stages, corresponding perfectly to the results of the present work, were observed by Jon *et al.* in α -brass at room temperature.⁹ The steep ADIF part at strain amplitudes higher than $\sim 10^{-4}$ was attributed to the activation of Frank-Read sources. According to Ref. 9, dislocation motion at higher strain amplitudes, with the IF leveled off, was controlled by viscous forces.

It appears that none of the different mechanisms suggested in Refs. 9 and 46 to account for very similar phenomena is applicable to our data. Considering the interpretation by Gottschall and Beshers,⁴⁶ we should mention the following points. First, the results reported in the present work are mostly for specimens prestrained at room temperature, in contrast to the data by Gottschall and Beshers for annealed crystals. No evidence of detectable pinning of fresh dislocations by atmospheres (time dependence of the ADIF, strain amplitude hysteresis, aging after deformation) is revealed in the present work at temperatures below ~ 300 K, nor in Refs. 39 and 40 for *in situ* ADIF measurements during deformation of Cu-Ni crystals. Thus, fresh dislocations free of PO atmospheres are responsible for the anelasticity of deformed crystals reported in the present work. In the following, we will show that atmospheres, indeed, form in Cu-Ni crystals as a result of high-temperature annealing, and we analyze their influence on the strain amplitude dependence of the IF, modulus defect and the friction stress acting on dislocations. Second, the absence of the retrapping of the dislocations by

atmospheres after the breakaway has been ascribed in Ref. 46 to inertial effects. However, inertial effects are efficient only when the viscous constant B is rather low (low temperatures, superconducting state of metals^{57,58}), and should be negligible at room temperature.

The basis for claiming that the activation of Frank-Read sources and the viscous friction were responsible for the steep ADIF part with a saturation was⁹ an increase of the ADMD, more pronounced than the ADIF, whereas the string breakaway model predicts their ratio to be ~ 1 , and therefore, the long-range dislocation motion was supposed; a qualitative similarity of the ADIF behavior with the phenomenological law, relating the dislocation velocity $v(\sigma)$ with the applied stress during unidirectional motion of dislocations in static experiments.

Several comments are needed regarding the arguments added.

a. Activation of Frank-Read sources. First, a complete reversibility of the strain amplitude dependence of the IF in prestrained crystals is typical both for the steep ADIF increase and the saturation range at low and high temperatures (see Fig. 1). This is a clear indication of the stability of the dislocation structure in our experiments, whereas a very pronounced hysteresis of the strain amplitude dependence is typical for the dislocation multiplication by vibrations (formation of slip lines) in annealed crystals.³⁶⁻³⁸ Second, the activation of Frank-Read sources is usually considered to be an athermal process. The microplastic ADIF which is due to dislocation multiplication or dislocation-dislocation interaction was reported to be practically temperature independent.⁵⁹ No data on temperature dependence of the steep ADIF stage, which might permit one to ascribe it to the athermal activation of Frank-Read sources, were reported in Ref. 9, whereas our results show a strong temperature dependence of this ADIF stage.

b. Viscous drag. The present data on the ADIF and ADMD, obtained in a wide temperature range and at different frequencies, allow us to verify also the hypothesis⁹ of viscous friction forces that control dislocation motion at the highest strain amplitudes (the ADIF saturation range). Figure 10 shows an analysis of the ADIF saturation for a Cu-1.3 at. % Ni crystal. The strain amplitude dependences of the decrement and the Young's modulus defect are shown in Fig. 10 for a frequency of ~ 100 kHz at 295 and 8 K. The strain amplitude dependence of the anelastic strain amplitude is deduced from the ADMD values according to Eq. (2). The intersecting straight lines show how the onset of ADIF saturation was determined, whereas the vertical arrows determine the corresponding values of anelastic strain amplitude. Clearly, the onset of ADIF saturation, at different temperatures, corresponds to approximately the same anelastic strain amplitude value (the same strain rate) for frequency of ~ 100 kHz. However, provided the ADIF saturation is due to the viscous friction, one should expect a strong influence of temperature on the strain rate at the onset of ADIF saturation, since the viscous friction constant, B , changes drastically with temperature. Additional evidence against the viscous friction mechanism of ADIF saturation can be obtained from the frequency dependence of the ADIF. The strain amplitude

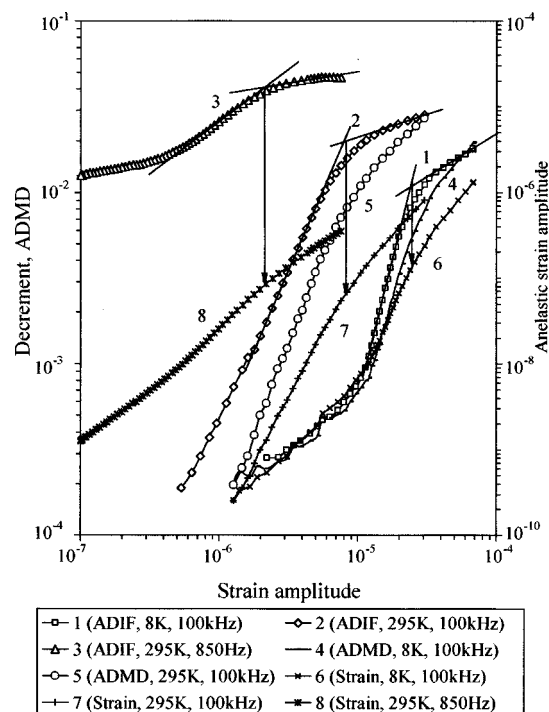


FIG. 10. Strain amplitude dependence of the decrement (1), (2), (3), the Young's modulus defect (4), (5) and anelastic strain amplitude (6), (7), (8) for a specimen of Cu-1.3 at. % Ni alloy at frequencies near 100 kHz (1), (2), (4), (5), (6), (7), 850 Hz (3), (8) and temperatures of 8 K (1), (4), (6) and 295 K (2), (3), (5), (7), (8). The intersections of the solid lines indicate how the onset of the ADIF saturation was determined; the vertical arrows show the anelastic strain amplitude at the onset of the ADIF saturation. The curve for the decrement at ~ 100 kHz and at 295 K is shown with a subtracted amplitude-independent component.

dependence of the decrement for an annealed specimen, taken at room temperature near 850 Hz, is seen in Fig. 10 as well. The data on the ADMD are not available at this frequency. However, as an estimation, the ADIF values can be used as a substitution for the ADMD in Eq. (2), since the ADIF and ADMD are of the same order of magnitude; see, for example, Fig. 9. The corresponding curve for the estimation of anelastic strain at ~ 850 Hz is also shown in Fig. 10. Apparently, ADIF saturation again occurs at nearly the same values of the anelastic strain amplitude, as at a frequency of ~ 100 kHz. As a consequence, the values of the anelastic strain rate, $\dot{\epsilon}_{an}$, corresponding to the onset of ADIF saturation, are approximately two orders of magnitude lower at 850 Hz than at 100 kHz. This observation also rules out viscous friction as the origin of ADIF saturation, since in that instance one should expect the occurrence of ADIF saturation at room temperature and different frequencies for the same anelastic strain rate values. Inasmuch as ADIF saturation is determined by anelastic strain rather than by the strain rate, it is likely not a dynamic effect.

c. ADIF to ADMD ratio. First, as analyzed in Sec. I, unlocalized friction IF models, rather than the string breakaway ones, are applicable in the case of concentrated solid solutions. Therefore, there is no point in referring to the ADIF to ADMD ratio predicted by the Granato-Lücke breakaway model. Models of the unlocalized friction type predict at high strain amplitudes, without assuming the dislocation

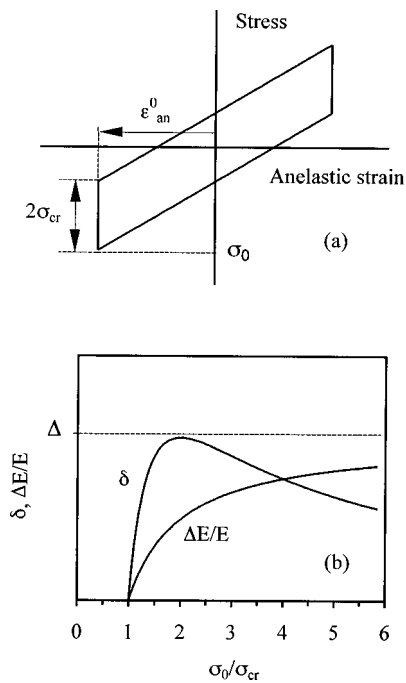


FIG. 11. Schematic representation of the stress-anelastic strain hysteresis (a) and strain amplitude dependence of the decrement and the Young's modulus defect (b), corresponding to the internal friction model of the unlocalized friction type. Δ represents the relaxation strength.

multiplication, the steep ADIF increase with saturation (maximum), accompanied by the monotonic ADMD increase (see, for example, Ref. 28). This type of the behavior corresponds qualitatively with the results in Ref. 9 and those in the present work (see Fig. 10). Second, considering the comparison of the ADIF and ADMD in Ref. 9, we should make the following general remark. It appears that the heating of specimens by ultrasound should be taken into consideration for the rather high strain amplitudes employed in Ref. 9. Consider, for example, the vibrations of a specimen with strain amplitude $\varepsilon_0 = 10^{-3}$ and $Q^{-1} = 3 \times 10^{-3}$ at a frequency of 20 kHz.⁹ The energy, dissipated in a cycle of vibrations in a unit volume of a specimen material, is given by $\Delta W = 2\pi Q^{-1}W$, where $W = E\varepsilon_0^2/2$ is the maximum value of the elastic energy of the vibrations. Under these circumstances, power $\Delta W \sim 20 \text{ W/cm}^3$ is dissipated in the specimen, sufficient to increase its temperature adiabatically by $\sim 5 \text{ K}$ in 1 s. Heating of the specimen may seemingly change the ADMD with increasing strain amplitude due to the temperature dependence of the elastic moduli. Heating usually influences the ADIF values to a lesser extent, thus changing the ADIF to ADMD ratio. Therefore, one should take special precautions to avoid the effect of heating the specimen on measured ADMD magnitudes when very high strain amplitudes are employed.

It appears that the ADIF and ADMD behavior observed in the present work at moderate and high strain amplitudes can be explained qualitatively using the simplest form of the unlocalized friction concept, which is often used to account for the ADIF in solid solutions.^{2,14-17} For the simplified model, represented schematically in Fig. 11, the onset of the ADIF corresponds to the condition $\sigma_0 = \sigma_{cr}$, where σ_{cr} is the

critical stress for the stationary thermally activated dislocation motion over an array of short-range obstacles. More pronounced ADIF saturation, compared to the ADMD behavior, is expected with a strain amplitude increase, when dislocation motion becomes progressively more controlled by the line tension. This tendency in the ADIF and ADMD behavior in the range of the ADIF saturation is, indeed, observed in our data; see Fig. 10.

For the unlocalized friction model, the critical stress is given by:²⁸

$$\sigma_{cr} = \frac{F_0}{Lb} \left[1 - \frac{kT}{U_0} \ln \left(\frac{\omega_0}{\omega} \right) \right]^\alpha,$$

where U_0 and F_0 are the maximum values of the activation energy and interaction force between a dislocation and a short-range obstacle, L and b are the average dislocation segment length and the magnitude of the Burgers vector, ω_0 and ω are the attack and applied angular frequencies, and $1 < \alpha < 2$ is a constant. Clearly, σ_{cr} is frequency, temperature and impurity concentration dependent. This dependence accounts qualitatively for the observed ADIF and ADMD behavior.

C. Friction stress acting on dislocations: Annealed and prestrained specimens

We suggest using the concept of the average friction stress acting on a dislocation to gain a better insight into the dislocation dynamics in the ADIF range. Suppose we have a stress-anelastic strain hysteresis of an arbitrary form, for the sake of simplicity, of the unlocalized friction type, Fig. 11. The energy dissipated in a cycle of vibrations in a unit volume corresponds to the area within the hysteresis loop: $\Delta W = \oint \sigma d\varepsilon$. We define the *average friction stress*, $\bar{\sigma}_f$, by $\Delta W = 4\bar{\sigma}_f \varepsilon_{an}^0$, where ε_{an}^0 is the anelastic strain amplitude. On the other hand, by definition, the strain amplitude-dependent decrement and the Young's modulus defect are $\delta_h = \Delta W/2W$ and $\Delta E/E = \varepsilon_{an}^0/\varepsilon_0$. Since the strain amplitude dependences of the IF and modulus defect are available from the experiment, one can easily deduce the average friction stress directly from the experimental data:

$$\bar{\sigma}_f = \frac{\Delta W}{4\varepsilon_{an}^0} = \frac{\delta_h}{\Delta E/E} \frac{E\varepsilon_0}{4},$$

or, in terms of the ADIF to ADMD ratio,

$$\bar{\sigma}_f = r \frac{E\varepsilon_0}{4}. \quad (5)$$

For example, in the case of a "simple hysteresis,"²² the average friction stress should exhibit a linear increase with the strain amplitude. The notion of friction stress acting on a moving dislocation in solid solution has been used in Refs. 10 and 14. The mean value of the frictional stress was deduced from the whole strain amplitude dependence of the decrement by fitting a certain phenomenological equation. In the present work we propose analyzing the stress amplitude dependence of the average friction stress.

Figure 12 shows how the average friction stress may be used to reveal the formation of pinning atmospheres as a

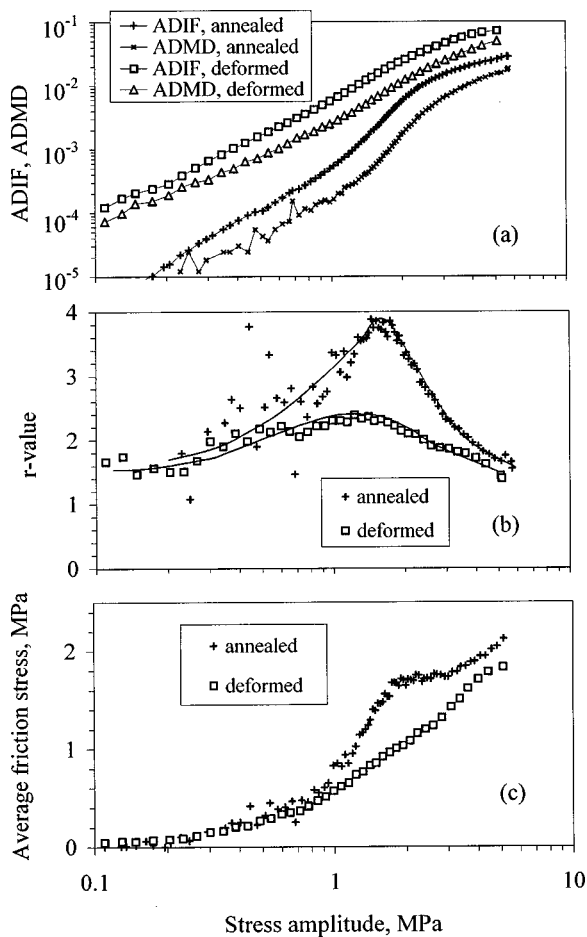


FIG. 12. Influence of annealing at 973 K and prestrain at room temperature on the stress amplitude dependence of the amplitude-dependent internal friction and the Young's modulus defect (a), their ratio (b), and average friction stress (c) for a Cu-2.3 at. % Ni specimen.

result of high-temperature annealing of a Cu-Ni crystal. Figure 12(a) represents the stress amplitude dependences of the IF and modulus defect for an initially annealed Cu-2.3 at. % Ni specimen. The stress amplitude, σ_0 , was derived from the elastic strain amplitude ϵ_0 using the measured value of the Young's modulus $E=136$ GPa for the Cu-2.3 at. % Ni crystal: $\sigma_0=\epsilon_0 \times E$. Similar results are depicted for the same specimen after deformation at room temperature in three-point bending. Figure 12(b) shows the stress amplitude dependence of the r value, whereas Fig. 12(c) represents the amplitude dependence of the average friction stress, calculated according to Eq. (5). As usual, three stages of ADIF and ADMD behavior can be discerned; see Fig. 12(a). Clearly, prestraining leads to an overall increase of the ADIF and ADMD. The ADIF and ADMD at the low-amplitude stage (below ~ 1 MPa) increase with prestrain to the greatest extent. However, the slope of the amplitude dependence on this stage is almost unchanged. At moderate stress amplitudes (1–3 MPa) both the ADIF values and the slope of the stress amplitude dependence change with prestrain. The amplitude dependences of the IF and modulus defect become more gradual after deformation of the specimen. We recall here that the same regularities have been found in the strain amplitude dependence of the annealed and deformed speci-

mens at low temperatures, Fig. 1(b): the athermal low-amplitude ADIF stage had the same slope for the annealed and deformed samples and for different Ni contents; deformation and Ni content influenced the absolute values of the ADIF at this stage; (2) the slope of the temperature-dependent ADIF stage at moderate strain amplitudes increased with Ni content, and was the highest for an annealed Cu-2.3 at. % Ni specimen.

Figure 12(b) shows that for the annealed specimen a pronounced maximum of the r value exists. The position of the maximum corresponds to the steep part of the stress amplitude dependence which occurs at stress amplitudes $\sim(1-3)$ MPa.

Finally, two observations merit closer attention to the behavior of the average friction stress, Fig. 12(c). First, the average friction stress is nearly the same for the annealed and deformed states at low and high stress amplitudes. Second, at moderate stress amplitudes, a kind of smooth maximum is observed for the annealed state. In the vicinity of this maximum, the friction stress is noticeably higher for the annealed than for the deformed state of the specimen.

The above mentioned regularities correspond fairly well with the suggested hierarchical model of the ADIF in solid solutions, if one assumes that high-temperature annealing (20 h at 973 K) leads to formation of pinning atmospheres around dislocations. It is reasonable to suggest that the atmospheres are not too extended and that they represent strong short-range obstacles for dislocations. According to the suggested model, the low-strain amplitude stage of the ADIF in solid solutions is mostly due to the interaction of dislocations with PO distributed in the bulk. Therefore, the formation of atmospheres does not influence the functional form of the ADIF on the low-strain amplitude stage, since the slope of the low-amplitude IF stage does not depend on the Ni content; see Fig. 1(b). In contrast, the formation of atmospheres strongly affects the steep ADIF stage at moderate stress amplitudes, which is supposed to be due to the dislocation interactions with the solute atoms situated close to the dislocation glide plane. In this stage the slope of the IF and the modulus defect stress amplitude dependence increases with Ni content, Figs. 1(b) and 4. The effect of the annealing is similar to the increase of the Ni content; see Figs. 1(b) and 12(a). This is an indication of a higher solute atom concentration around the dislocations in the annealed state. Apparently, interaction of dislocations with the solute atoms forming the atmospheres leads to an increase of the friction stress at moderate stress amplitudes, Fig. 12(c). At higher stress amplitudes, when dislocation motion occurs on a larger scale, the contribution of atmospheres becomes less significant, and the friction stress for the annealed and deformed states again attains the same values, Fig. 12(c).

Thus, the suggested qualitative model accounts also for the difference in the ADIF of prestrained and annealed crystals.

D. Qualitative model for temperature/frequency dependence of the ADIF in solid solutions

As stated above, the ADIF at low strain amplitudes, low temperatures and high frequencies is predominantly due to

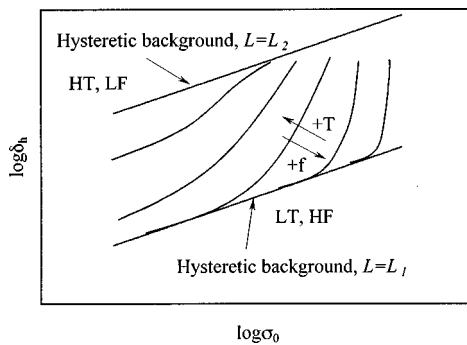


FIG. 13. Schematic representation of the influence of temperature and frequency on the amplitude-dependent internal friction in solid solutions.

the athermal motion of dislocations over long-range obstacles distributed in the bulk of a crystal. However, the presence of weak long-range obstacles should also influence the ADIF behavior at moderate and high strain amplitudes. This influence should be especially pronounced at high temperatures and low frequencies, when short-range strong obstacles become progressively weaker. Schematically, the influence of temperature and frequency on both the low-amplitude IF and the ADIF at moderate and high strain amplitudes can be seen in Fig. 13. One expects that, at very high temperatures/low frequencies, the motion of dislocations is again governed by weak athermal obstacles, even at rather high strain amplitudes. It is remarkable that in this limiting case the strain amplitude dependence of the IF transforms in the whole range of strain amplitudes into a strain amplitude-dependent hysteretic damping determined by an average loop length L_2 , much higher than that at low temperatures/high frequencies, L_1 . It means that the frequency- and temperature-dependent steep ADIF component should diminish with increasing temperature/decreasing frequency. Apparently, the experimental data in Fig. 8 correspond qualitatively with the hypothesis suggested. We should mention here that the proposed analysis does not account for possible contributions of larger scales of the defect structure, which might become important at high values of anelastic strain (high temperatures, low frequencies). For instance, dislocation-dislocation interactions can contribute considerably to the ADIF.³⁻⁷

V. CONCLUSIONS

Detailed experimental investigations of the ADIF, ADMD and dislocation anelastic strain in single crystals of the Cu-Ni system in wide temperature and strain amplitude ranges and at different frequencies reveal the existence of several stages of dislocation microplasticity. These stages are ascribed to the athermal and thermally activated motion of dislocations over stress fields of solute atoms.

The variety of the experimental observations can be explained self-consistently considering dislocation motion in the two-component array of the PO. The distinctive feature of the present approach is the assumption that weak obstacles are long range and athermal ones, whereas strong obstacles are short range and can be overcome with the assistance of thermal activation. These types of dislocation-PO interac-

tions correspond to the solute atoms distributed in the bulk of a crystal and in the dislocation glide plane respectively.

A qualitative explanation for the formation of the low-amplitude IF background in solid solutions in different temperature and frequency ranges has been suggested. Two asymptotic ranges are expected where the ADIF should exhibit temperature- and frequency-independent behavior.

Low temperatures, high frequencies. Here, the hysteretic IF background should be observed due to the dislocation motion over weak obstacles. The average dislocation loop length is determined by the strong short-range obstacles, which can be overcome at higher strain amplitudes, producing the temperature- and frequency-dependent ADIF stage.

High temperatures, low frequencies. The ADIF in this domain is again mostly due to the dislocation motion over weak long-range obstacles. However, the ADIF here should attain much higher values due to the increase of the average loop length. The steep temperature- and frequency-dependent ADIF stage should diminish in this domain, making the ADIF again frequency and temperature independent in a wide range of strain amplitudes.

A more detailed microscopic model is under development.

ACKNOWLEDGMENTS

The partial support from the Swiss National Science Foundation in the framework of IP Project No. 71P 051832 is gratefully acknowledged. The authors are grateful to F. Hutson for careful reading of the manuscript.

- ¹A. S. Nowick and B. S. Berry, *Anelastic Relaxation in Crystalline Solids* (Academic, New York, 1972).
- ²G. Gremaud, in *Mechanical Spectroscopy and its Application to Material Science*, edited by L. B. Magalas (Elsevier Applied Science, England, to be published).
- ³J. Dralla and J. C. Bilello, *J. Appl. Phys.* **41**, 2340 (1970).
- ⁴D. G. Pinatti and J. M. Roberts, *J. Appl. Phys.* **53**, 933 (1982).
- ⁵J. M. Roberts, *Phys. Status Solidi A* **19**, 731 (1973); **20**, 145 (1973).
- ⁶S. N. Golyandin and S. B. Kustov, *Phys. Solid State* **34**, 2031 (1992); **34**, 2035 (1992); **37**, 1786 (1995).
- ⁷S. Kustov and S. Golyandin, *ASTM STP N 1304*, 1997, p. 22.
- ⁸A. V. Granato and K. Lücke, *J. Appl. Phys.* **27**, 583 (1956); **27**, 789 (1956).
- ⁹M. C. Jon, W. P. Mason, and D. N. Beshers, *J. Appl. Phys.* **47**, 2337 (1976).
- ¹⁰V. A. Chelnokov and N. L. Kuz'min, *Sov. Phys. Solid State* **22**, 1751 (1980).
- ¹¹O. Boser, *J. Appl. Phys.* **54**, 2338 (1983).
- ¹²Y. Nishino, Y. Okada, and S. Asano, *Phys. Status Solidi A* **129**, 409 (1992).
- ¹³J. C. Swartz and J. Weertman, *J. Appl. Phys.* **32**, 1860 (1961).
- ¹⁴V. A. Chelnokov, V. A. Stepanov, and N. L. Kuz'min, *Sov. Phys. Solid State* **12**, 649 (1970).
- ¹⁵H. Araki and T. Ninomiya, *J. Phys. Soc. Jpn.* **41**, 1684 (1976).
- ¹⁶I. G. Ritchie, A. Atrens, C. B. So, and K. W. Sprungmann, *J. Phys. Colloq.* **42**, C5 (1981).
- ¹⁷J. Schlipf, in *Proceedings of the 6th International Conference on Internal Friction and Ultrasonic Attenuation in Solids*, edited by R. R. Hasiguti and N. Mikoshiba (University of Tokyo Press, Tokyo, 1977), p. 91.
- ¹⁸K. Ishii, *J. Phys. Soc. Jpn.* **52**, 149 (1983).
- ¹⁹G. D'Anna, W. Benoit, and V. Vinokur, *J. Appl. Phys.* **82**, 5983 (1997).
- ²⁰K. Ishii, in *Proceedings of the 9th International Conference on Internal Friction and Ultrasonic Attenuation in Solids, Beijing, 1989*, edited by T. S. Kê (IAP, Pergamon, Oxford, 1990), p. 45.
- ²¹K. Ishii, *J. Alloys Compd.* **211/212**, 173 (1994).
- ²²A. S. Nowick, *Phys. Rev.* **80**, 249 (1950).

- ²³S. Takahashi, J. Phys. Soc. Jpn. **11**, 1253 (1956).
- ²⁴S. Weinig and E. S. Machlin, J. Appl. Phys. **27**, 734 (1956).
- ²⁵J. L. Routbort and H. S. Sack, J. Appl. Phys. **37**, 4803 (1966).
- ²⁶J. Baur and W. Benoit, J. Appl. Phys. **60**, 3473 (1986).
- ²⁷J. Baur and W. Benoit, J. Appl. Phys. **61**, 2463 (1987).
- ²⁸G. Gremaud, J. Phys. Colloq. **48**, C8 (1985).
- ²⁹F. E. Rowett, Proc. R. Soc. London, Ser. A **87**, 502 (1912).
- ³⁰T. A. Read, Phys. Rev. **58**, 371 (1940).
- ³¹Y. Hiki, J. Phys. Soc. Jpn. **13**, 1138 (1958).
- ³²S. B. Kustov, J. Van Humbeeck, I. Hurtado, S. N. Golyandin, and R. De Batist, ASTM STP N 1304, 1997, p. 94.
- ³³G. Gremaud and S. Kustov, Phys. Rev. B. (submitted).
- ³⁴W. H. Robinson and A. Edgar, IEEE Trans. Sonics Ultrason. **SU-21**, 98 (1974).
- ³⁵S. B. Kustov, B. K. Kardashev, and V. I. Ivanov, *et al.*, Preprint FEI-2141 (FEI, Obninsk, 1990) (in Russian).
- ³⁶V. A. Chelnokov and N. L. Kuz'min, Sov. Phys. Solid State **24**, 1796 (1982).
- ³⁷B. I. Smirnov, V. A. Chelnokov, and N. L. Kuz'min, Sov. Phys. Solid State **25**, 293 (1983).
- ³⁸T. Nakamura and K. Ishii, in *Proceedings of the 5th International Conference on Internal Friction and Ultrasonic Attenuation in Solids*, edited by D. Lenz and K. Lücke (Springer, Berlin, 1975), Vol. 2, p. 478.
- ³⁹S. Golyandin, K. Sapozhnikov, S. Kustov, Y. Nishino, and S. Asano, J. Phys. IV **6**, C8 (1996).
- ⁴⁰K. V. Sapozhnikov, S. N. Golyandin, S. B. Kustov, Y. Nishino, and S. Asano, Philos. Mag. A **77**, 151 (1998).
- ⁴¹C. Zener, *Elasticity and Anelasticity of Metals* (Chicago, 1948).
- ⁴²*Tables of Physical Quantities. Handbook*, edited by I. K. Kikoin (Atomizdat, Moscow, 1976) (in Russian).
- ⁴³B. J. Lazan, *Damping of Materials and Members in Structural Mechanics* (Pergamon, New York, 1968).
- ⁴⁴S. Asano, Philos. Mag. **30**, 1155 (1974).
- ⁴⁵G. Fantozzi, C. Esnouf, W. Benoit, and I. G. Ritchie, Prog. Mater. Sci. **27**, 311 (1982).
- ⁴⁶R. J. Gottschall and D. N. Beshers, J. Appl. Phys. **48**, 5074 (1977).
- ⁴⁷S. Asano, J. Phys. Soc. Jpn. **29**, 952 (1970).
- ⁴⁸S. Kustov, S. Golyandin, J. Van Humbeeck, and R. De Batist, J. Phys. IV **6**, C8 (1996).
- ⁴⁹S. Kustov, S. Golyandin, K. Sapozhnikov, J. Van Humbeeck, and R. De Batist, Acta Mater. **46**, 5117 (1998).
- ⁵⁰J. Lauzier, M. Ory, G. Fantozzi, C. Minier, and P. Moser, Phys. Status Solidi A **32**, 305 (1975).
- ⁵¹C. Bonjour and W. Benoit, Acta Metall. **27**, 1755 (1979).
- ⁵²J. Ni and J. Schlipf, in Ref. 20, p. 53.
- ⁵³S. B. Kustov, Ph.D. thesis, A. F. Ioffe Physico-Technical Institute, Leningrad, USSR, 1989.
- ⁵⁴A. B. Lebedev and S. B. Kustov, Phys. Status Solidi A **136**, K85 (1993).
- ⁵⁵A. B. Lebedev, Philos. Mag. A **74**, 137 (1996).
- ⁵⁶R. Gotthardt, J. Phys. Colloq. **43**, C4 (1982).
- ⁵⁷A. V. Granato, Phys. Rev. B **4**, 2196 (1971).
- ⁵⁸R. D. Isaac, R. B. Schwarz, and A. V. Granato, Phys. Rev. B **18**, 4143 (1978).
- ⁵⁹S. Golyandin, S. Kustov, K. Sapozhnikov *et al.*, Phys. Solid State (in press).